First Measurement of the Decay Asymmetry of pure W-exchange Decay $\Lambda_c^+ \to \Xi^0 K^+$

M. Ablikim[1], M. N. Achasov[4,b], P. Adlarson[75], O. Afedulidis[3], X. C. Ai[80], R. Aliberti[35], A. Amoroso[74A,74C], Q. An[71,58], Y. Bai[57], O. Bakina[36], I. Balossino[29A], Y. Ban[46,g], H.-R. Bao[63], V. Batozskaya[1,44], K. Begzsuren[32], N. Berger[35], M. Berlowski[44], M. Bertani[28A], D. Bettoni[29A], F. Bianchi[74A,74C], E. Bianco[74A,74C], A. Bortone[74A,74C], I. Boyko[36], R. A. Briere[5], A. Brueggemann[68], H. Cai[76], X. Cai[1,58], A. Calcaterra[28A], G. F. Cao[1,63], N. Cao[1,63], S. A. Cetin[62A], J. F. Chang[1,58], W. L. Chang[1,63], G. R. Che[43], G. Chelkov[36,a], C. Chen[43], C. H. Chen[9], Chao Chen[55], G. Chen[1], H. S. Chen[1,63], M. L. Chen[1,58,63], S. J. Chen[42], S. L. Chen[45], S. M. Chen[61], T. Chen[1,63], X. R. Chen[31,63], X. T. Chen[1,63], Y. B. Chen[1,58], Y. Q. Chen[34], Z. J. Chen[25,h], Z. Y. Chen[1,63], S. K. Choi[10A], X. Chu[43], G. Cibinetto[29A], F. Cossio[74C], J. J. Cui[50], H. L. Dai[1,58], J. P. Dai[78], A. Dbeyssi[18], R. E. de Boer[3], D. Dedovich[36], C. Q. Deng[72], Z. Y. Deng[1], A. Denig[35], I. Denysenko[36], M. Destefanis[74A,74C], F. De Mori[74A,74C], B. Ding[66,1], X. X. Ding[46,g], Y. Ding[34], Y. Ding[40], J. Dong[1,58], L. Y. Dong[1,63], M. Y. Dong[1,58,63], X. Dong[76], M. C. Du[1], S. X. Du[80], Z. H. Duan[42], P. Egorov[36,a], Y. H. Fan[45], J. Fang[59], J. Fang[1,58], S. S. Fang[1,63], W. X. Fang[1], Y. Fang[1], Y. Q. Fang[1,58], R. Farinelli[29A], L. Fava[74B,74C], F. Feldbauer[3], G. Felici[28A], C. Q. Feng[71,58], J. H. Feng[59], Y. T. Feng[71,58], K. Fischer[69], M. Fritsch[3], C. D. Fu[1], J. L. Fu[63], Y. W. Fu[1], H. Gao[63], Y. N. Gao[46,g], Yang Gao[71,58], S. Garbolino[74C], I. Garzia[29A,29B], P. T. Ge[76], Z. W. Ge[42], C. Geng[59], E. M. Gersabeck[67], A. Gilman[69], K. Goetzen[13], L. Gong[40], W. X. Gong[1,58], W. Gradl[35], S. Gramigna[29A,29B], M. Greco[74A,74C], M. H. Gu[1,58], Y. T. Gu[15], C. Y. Guan[1,63], Z. L. Guan[22], A. Q. Guo[31,63], L. B. Guo[41], M. J. Guo[50], R. P. Guo[49], Y. P. Guo[12,f], A. Guskov[36,a], J. Gutierrez[27], K. L. Han[63], T. T. Han[1], X. Q. Hao[19], F. A. Harris[65], K. K. He[55], K. L. He[1,63], F. H. Heinsius[3], C. H. Heinz[35], Y. K. Heng[1,58,63], C. Herold[60], T. Holtmann[3], P. C. Hong[12,f], G. Y. Hou[1,63], X. T. Hou[1,63], Y. R. Hou[63], Z. L. Hou[1], B. Y. Hu[59], H. M. Hu[1,63], J. F. Hu[56,i], T. Hu[1,58,63], Y. Hu[1], G. S. Huang[71,58], K. X. Huang[59], L. Q. Huang[31,63], X. T. Huang[50], Y. P. Huang[1], T. Hussain[73], F. Hölzken[3], N Hüsken[27,35], N. in der Wiesche[68], M. Irshad[71,58], J. Jackson[27], S. Janchiv[32], J. H. Jeong[10A], Q. Ji[1], Q. P. Ji[19], W. Ji[1,63], X. B. Ji[1,63], X. L. Ji[1,58], Y. Y. Ji[50], X. Q. Jia[50], Z. K. Jia[71,58], D. Jiang[1,63], H. B. Jiang[76], P. C. Jiang[46,g], S. S. Jiang[39], T. J. Jiang[16], X. S. Jiang[1,58,63], Y. Jiang[63], J. B. Jiao[50], J. K. Jiao[34], Z. Jiao[23], S. Jin[42], Y. Jin[66], M. Q. Jing[1,63], X. M. Jing[63], T. Johansson[75], S. Kabana[33], N. Kalantar-Nayestanaki[64], X. L. Kang[9], X. S. Kang[40], M. Kavatsyuk[64], B. C. Ke[80], V. Khachatryan[27], A. Khoukaz[68], R. Kiuchi[1], O. B. Kolcu[62A], B. Kopf[3], M. Kuessner[3], X. Kui[1,63], A. Kupsc[44,75], W. Kühn[37], J. J. Lane[67], P. Larin[18], L. Lavezzi[74A,74C], T. T. Lei[71,58], Z. H. Lei[71,58], M. Lellmann[35], T. Lenz[35], C. Li[43], C. Li[47], C. H. Li[39], Cheng Li[71,58], D. M. Li[80], F. Li[1,58], G. Li[1], H. Li[71,58], H. B. Li[1,63], H. J. Li[19], H. N. Li[56,i], Hui Li[43], J. R. Li[61], J. S. Li[59], Ke Li[1], L. J Li[1,63], L. K. Li[1], Lei Li[48], M. H. Li[43], P. R. Li[38,k], Q. M. Li[1,63], Q. X. Li[50], R. Li[17,31], S. X. Li[12], T. Li[50], W. D. Li[1,63], W. G. Li[1], X. Li[1,63], X. H. Li[71,58], X. L. Li[50], Xiaoyu Li[1,63], Y. G. Li[46,g], Z. J. Li[59], Z. X. Li[15], C. Liang[42], H. Liang[1,63], H. Liang[71,58], Y. F. Liang[54], Y. T. Liang[31,63], G. R. Liao[14], L. Z. Liao[50], Y. P. Liao[1,63], J. Libby[26], A. Limphirat[60], D. X. Lin[31,63], T. Lin[1], B. J. Liu[1], B. X. Liu[76], C. Liu[34], C. X. Liu[1], F. H. Liu[53], Fang Liu[1], Feng Liu[6], G. M. Liu[56,i], H. Liu[38,j,k], H. B. Liu[15], H. M. Liu[1,63], Huanhuan Liu[1], Huihui Liu[21], J. B. Liu[71,58], J. Y. Liu[1,63], K. Liu[38,j,k], K. Y. Liu[40], Ke Liu[22], L. Liu[71,58], L. C. Liu[43], Lu Liu[43], M. H. Liu[12,f], P. L. Liu[1], Q. Liu[63], S. B. Liu[71,58], T. Liu[12,f], W. K. Liu[43], W. M. Liu[71,58], X. Liu[38,j,k], X. Liu[39], Y. Liu[80], Y. Liu[38,j,k], Y. B. Liu[43], Z. A. Liu[1,58,63], Z. D. Liu[9], Z. Q. Liu[50], X. C. Lou[1,58,63], F. X. Lu[59], H. J. Lu[23], J. G. Lu[1,58], X. L. Lu[1], Y. Lu[7], Y. P. Lu[1,58], Z. H. Lu[1,63], C. L. Luo[41], M. X. Luo[79], T. Luo[12,f], X. L. Luo[1,58], X. R. Lyu[63], Y. F. Lyu[43], F. C. Ma[40], H. Ma[78], H. L. Ma[1], J. L. Ma[1,63], L. L. Ma[50], M. M. Ma[1,63], Q. M. Ma[1], R. Q. Ma[1,63], X. T. Ma[1,63], X. Y. Ma[1,58], Y. Ma[46,g], Y. M. Ma[31], F. E. Maas[18], M. Maggiora[74A,74C], S. Malde[69], A. Mangoni[28B], Y. J. Mao[46,g], Z. P. Mao[1], S. Marcello[74A,74C], Z. X. Meng[66], J. G. Messchendorp[13,64], G. Mezzadri[29A], H. Miao[1,63], T. J. Min[42], R. E. Mitchell[27], X. H. Mo[1,58,63], B. Moses[27], N. Yu. Muchnoi[4,b], J. Muskalla[35], Y. Nefedov[36], F. Nerling[18,d], I. B. Nikolaev[4,b], Z. Ning[1,58], S. Nisar[11,l], Q. L. Niu[38,j,k], W. D. Niu[55], Y. Niu[50], S. L. Olsen[63], Q. Ouyang[1,58,63], S. Pacetti[28B,28C], X. Pan[55], Y. Pan[57], A. Pathak[34], P. Patteri[28A], Y. P. Pei[71,58], M. Pelizaeus[3], H. P. Peng[71,58], Y. Y. Peng[38,j,k], K. Peters[13,d], J. L. Ping[41], R. G. Ping[1,63], S. Plura[35], V. Prasad[33], F. Z. Qi[1], H. Qi[71,58], H. R. Qi[61], M. Qi[42], T. Y. Qi[12,f], S. Qian[1,58], W. B. Qian[63], C. F. Qiao[63], J. J. Qin[72], L. Q. Qin[14], X. S. Qin[50], Z. H. Qin[1,58], J. F. Qiu[1], S. Q. Qu[61], Z. H. Qu[72], C. F. Redmer[35], K. J. Ren[39], A. Rivetti[74C], M. Rolo[74C], G. Rong[1,63], Ch. Rosner[18], S. N. Ruan[43], N. Salone[44], A. Sarantsev[36,c], Y. Schelhaas[35], K. Schoenning[75], M. Scodeggio[29A], K. Y. Shan[12,f], W. Shan[24], X. Y. Shan[71,58], J. F. Shangguan[55], L. G. Shao[1,63], M. Shao[71,58], C. P. Shen[12,f], H. F. Shen[1,63], W. H. Shen[63], X. Y. Shen[1,63], B. A. Shi[63], H. C. Shi[71,58], J. L. Shi[12], J. Y. Shi[1], Q. Q. Shi[55], R. S. Shi[1,63], S. Y. Shi[72], X. Shi[1,58], J. J. Song[19], T. Z. Song[59], W. M. Song[34,1], Y. J. Song[12], S. Sosio[74A,74C], S. Spataro[74A,74C], F. Stieler[35], Y. J. Su[63], G. B. Sun[76], G. X. Sun[1], H. Sun[63], H. K. Sun[1], J. F. Sun[19], K. Sun[61], L. Sun[76], S. S. Sun[1,63], T. Sun[51,e], W. Y. Sun[34], Y. Sun[9], Y. J. Sun[71,58], Y. Z. Sun[1], Z. Q. Sun[1,63], Z. T. Sun[50], C. J. Tang[54], G. Y. Tang[1], J. Tang[59], Y. A. Tang[76], L. Y. Tao[72], Q. T. Tao[25,h], M. Tat[69], J. X. Teng[71,58], V. Thoren[75], W. H. Tian[59], Y. Tian[31,63], Z. F. Tian[76], I. Uman[62B], Y. Wan[55], S. J. Wang[50], B. Wang[1], B. L. Wang[63], Bo Wang[71,58], D. Y. Wang[46,g], F. Wang[72], H. J. Wang[38,j,k], J. P. Wang[50], K. Wang[1,58], L. L. Wang[1], M. Wang[50], Meng Wang[1,63], N. Y. Wang[63], S. Wang[12,f], S. Wang[38,j,k], T. Wang[12,f], T. J. Wang[43], W. Wang[72], W. Wang[59], W. P. Wang[71,58], X. Wang[46,g], X. F. Wang[38,j,k], X. J. Wang[39], X. L. Wang[12,f], X. N. Wang[1], Y. Wang[61], Y. D. Wang[45], Y. F. Wang[1,58,63], Y. L. Wang[19], Y. N. Wang[45], Y. Q. Wang[1], Yaqian Wang[17], Yi Wang[61], Z. Wang[1,58], Z. L. Wang[72], Z. Y. Wang[1,63], Ziyi Wang[63], D. Wei[70], D. H. Wei[14], F. Weidner[68], S. P. Wen[1], Y. R. Wen[39], U. Wiedner[3], G. Wilkinson[69], M. Wolke[75], L. Wollenberg[3], C. Wu[39], J. F. Wu[1,8], L. H. Wu[1], L. J. Wu[1,63], X. Wu[12,f], X. H. Wu[34], Y. Wu[71], Y. H. Wu[55], Y. J. Wu[31], Z. Wu[1,58], L. Xia[71,58], X. M. Xian[39], B. H. Xiang[1,63], T. Xiang[46,g], D. Xiao[38,j,k], G. Y. Xiao[42], S. Y. Xiao[1], Y. L. Xiao[12,f], Z. J. Xiao[41], C. Xie[42], X. H. Xie[46,g], Y. Xie[50], Y. G. Xie[1,58], Y. H. Xie[6], Z. P. Xie[71,58], T. Y. Xing[1,63], C. F. Xu[1,63], C. J. Xu[59], G. F. Xu[1], H. Y. Xu[66], Q. J. Xu[16], Q. N. Xu[30], W. Xu[1], W. L. Xu[66], X. P. Xu[55], Y. C. Xu[77], Z. P. Xu[42], Z. S. Xu[63], F. Yan[12,f], L. Yan[12,f], W. B. Yan[71,58], W. C. Yan[80], X. Q. Yan[1], H. J. Yang[51,e], H. L. Yang[34], H. X. Yang[1],

Tao Yang[1], Y. Yang[12,f], Y. F. Yang[43], Y. X. Yang[1,63], Yifan Yang[1,63], Z. W. Yang[38,j,k], Z. P. Yao[50], M. Ye[1,58], M. H. Ye[8], J. H. Yin[1], Z. Y. You[59], B. X. Yu[1,58,63], C. X. Yu[43], G. Yu[1,63], J. S. Yu[25,h], T. Yu[72], X. D. Yu[46,g], C. Z. Yuan[1,63], J. Yuan[34], L. Yuan[2], S. C. Yuan[1], Y. Yuan[1,63], Z. Y. Yuan[59], C. X. Yue[39], A. A. Zafar[73], F. R. Zeng[50], S. H. Zeng[72], X. Zeng[12,f], Y. Zeng[25,h], Y. J. Zeng[59], Y. J. Zeng[1,63], X. Y. Zhai[34], Y. C. Zhai[50], Y. H. Zhan[59], A. Q. Zhang[1,63], B. L. Zhang[1,63], B. X. Zhang[1], D. H. Zhang[43], G. Y. Zhang[19], H. Zhang[71], H. C. Zhang[1,58,63], H. H. Zhang[59], H. H. Zhang[34], H. Q. Zhang[1,58,63], H. Y. Zhang[1,58], J. Zhang[59], J. Zhang[80], J. J. Zhang[52], J. L. Zhang[20], J. Q. Zhang[41], J. W. Zhang[1,58,63], J. X. Zhang[38,j,k], J. Y. Zhang[1], J. Z. Zhang[1,63], Jianyu Zhang[63], L. M. Zhang[61], Lei Zhang[42], P. Zhang[1,63], Q. Y. Zhang[39,80], Shuihan Zhang[1,63], Shulei Zhang[25,h], X. D. Zhang[45], X. M. Zhang[1], X. Y. Zhang[50], Y. Zhang[72], Y. T. Zhang[80], Y. H. Zhang[1,58], Y. M. Zhang[39], Yan Zhang[71,58], Yao Zhang[1], Z. D. Zhang[1], Z. H. Zhang[1], Z. L. Zhang[34], Z. Y. Zhang[76], Z. Y. Zhang[43], G. Zhao[1], J. Y. Zhao[1,63], J. Z. Zhao[1,58], Lei Zhao[71,58], Ling Zhao[1], M. G. Zhao[43], R. P. Zhao[63], S. J. Zhao[80], Y. B. Zhao[1,58], Y. X. Zhao[31,63], Z. G. Zhao[71,58], A. Zhemchugov[36,a], B. Zheng[72], J. P. Zheng[1,58], W. J. Zheng[1,63], Y. H. Zheng[63], B. Zhong[41], X. Zhong[59], H. Zhou[50], J. Y. Zhou[34], L. P. Zhou[1,63], X. Zhou[76], X. K. Zhou[6], X. R. Zhou[71,58], X. Y. Zhou[39], Y. Z. Zhou[12,f], J. Zhu[43], K. Zhu[1], K. J. Zhu[1,58,63], L. Zhu[34], L. X. Zhu[63], S. H. Zhu[70], S. Q. Zhu[42], T. J. Zhu[12,f], W. J. Zhu[12,f], Y. C. Zhu[71,58], Z. A. Zhu[1,63], J. H. Zou[1], J. Zu[71,58]

(BESIII Collaboration)

[1] *Institute of High Energy Physics, Beijing 100049, People's Republic of China*
[2] *Beihang University, Beijing 100191, People's Republic of China*
[3] *Bochum Ruhr-University, D-44780 Bochum, Germany*
[4] *Budker Institute of Nuclear Physics SB RAS (BINP), Novosibirsk 630090, Russia*
[5] *Carnegie Mellon University, Pittsburgh, Pennsylvania 15213, USA*
[6] *Central China Normal University, Wuhan 430079, People's Republic of China*
[7] *Central South University, Changsha 410083, People's Republic of China*
[8] *China Center of Advanced Science and Technology, Beijing 100190, People's Republic of China*
[9] *China University of Geosciences, Wuhan 430074, People's Republic of China*
[10] *Chung-Ang University, Seoul, 06974, Republic of Korea*
[11] *COMSATS University Islamabad, Lahore Campus, Defence Road, Off Raiwind Road, 54000 Lahore, Pakistan*
[12] *Fudan University, Shanghai 200433, People's Republic of China*
[13] *GSI Helmholtzcentre for Heavy Ion Research GmbH, D-64291 Darmstadt, Germany*
[14] *Guangxi Normal University, Guilin 541004, People's Republic of China*
[15] *Guangxi University, Nanning 530004, People's Republic of China*
[16] *Hangzhou Normal University, Hangzhou 310036, People's Republic of China*
[17] *Hebei University, Baoding 071002, People's Republic of China*
[18] *Helmholtz Institute Mainz, Staudinger Weg 18, D-55099 Mainz, Germany*
[19] *Henan Normal University, Xinxiang 453007, People's Republic of China*
[20] *Henan University, Kaifeng 475004, People's Republic of China*
[21] *Henan University of Science and Technology, Luoyang 471003, People's Republic of China*
[22] *Henan University of Technology, Zhengzhou 450001, People's Republic of China*
[23] *Huangshan College, Huangshan 245000, People's Republic of China*
[24] *Hunan Normal University, Changsha 410081, People's Republic of China*
[25] *Hunan University, Changsha 410082, People's Republic of China*
[26] *Indian Institute of Technology Madras, Chennai 600036, India*
[27] *Indiana University, Bloomington, Indiana 47405, USA*
[28] *INFN Laboratori Nazionali di Frascati , (A)INFN Laboratori Nazionali di Frascati, I-00044, Frascati, Italy; (B)INFN Sezione di Perugia, I-06100, Perugia, Italy; (C)University of Perugia, I-06100, Perugia, Italy*
[29] *INFN Sezione di Ferrara, (A)INFN Sezione di Ferrara, I-44122, Ferrara, Italy; (B)University of Ferrara, I-44122, Ferrara, Italy*
[30] *Inner Mongolia University, Hohhot 010021, People's Republic of China*
[31] *Institute of Modern Physics, Lanzhou 730000, People's Republic of China*
[32] *Institute of Physics and Technology, Peace Avenue 54B, Ulaanbaatar 13330, Mongolia*
[33] *Instituto de Alta Investigación, Universidad de Tarapacá, Casilla 7D, Arica 1000000, Chile*
[34] *Jilin University, Changchun 130012, People's Republic of China*
[35] *Johannes Gutenberg University of Mainz, Johann-Joachim-Becher-Weg 45, D-55099 Mainz, Germany*
[36] *Joint Institute for Nuclear Research, 141980 Dubna, Moscow region, Russia*
[37] *Justus-Liebig-Universitaet Giessen, II. Physikalisches Institut, Heinrich-Buff-Ring 16, D-35392 Giessen, Germany*
[38] *Lanzhou University, Lanzhou 730000, People's Republic of China*
[39] *Liaoning Normal University, Dalian 116029, People's Republic of China*
[40] *Liaoning University, Shenyang 110036, People's Republic of China*
[41] *Nanjing Normal University, Nanjing 210023, People's Republic of China*
[42] *Nanjing University, Nanjing 210093, People's Republic of China*
[43] *Nankai University, Tianjin 300071, People's Republic of China*
[44] *National Centre for Nuclear Research, Warsaw 02-093, Poland*
[45] *North China Electric Power University, Beijing 102206, People's Republic of China*

[46] *Peking University, Beijing 100871, People's Republic of China*
[47] *Qufu Normal University, Qufu 273165, People's Republic of China*
[48] *Renmin University of China, Beijing 100872, People's Republic of China*
[49] *Shandong Normal University, Jinan 250014, People's Republic of China*
[50] *Shandong University, Jinan 250100, People's Republic of China*
[51] *Shanghai Jiao Tong University, Shanghai 200240, People's Republic of China*
[52] *Shanxi Normal University, Linfen 041004, People's Republic of China*
[53] *Shanxi University, Taiyuan 030006, People's Republic of China*
[54] *Sichuan University, Chengdu 610064, People's Republic of China*
[55] *Soochow University, Suzhou 215006, People's Republic of China*
[56] *South China Normal University, Guangzhou 510006, People's Republic of China*
[57] *Southeast University, Nanjing 211100, People's Republic of China*
[58] *State Key Laboratory of Particle Detection and Electronics, Beijing 100049, Hefei 230026, People's Republic of China*
[59] *Sun Yat-Sen University, Guangzhou 510275, People's Republic of China*
[60] *Suranaree University of Technology, University Avenue 111, Nakhon Ratchasima 30000, Thailand*
[61] *Tsinghua University, Beijing 100084, People's Republic of China*
[62] *Turkish Accelerator Center Particle Factory Group, (A)Istinye University, 34010, Istanbul, Turkey; (B)Near East University, Nicosia, North Cyprus, 99138, Mersin 10, Turkey*
[63] *University of Chinese Academy of Sciences, Beijing 100049, People's Republic of China*
[64] *University of Groningen, NL-9747 AA Groningen, The Netherlands*
[65] *University of Hawaii, Honolulu, Hawaii 96822, USA*
[66] *University of Jinan, Jinan 250022, People's Republic of China*
[67] *University of Manchester, Oxford Road, Manchester, M13 9PL, United Kingdom*
[68] *University of Muenster, Wilhelm-Klemm-Strasse 9, 48149 Muenster, Germany*
[69] *University of Oxford, Keble Road, Oxford OX13RH, United Kingdom*
[70] *University of Science and Technology Liaoning, Anshan 114051, People's Republic of China*
[71] *University of Science and Technology of China, Hefei 230026, People's Republic of China*
[72] *University of South China, Hengyang 421001, People's Republic of China*
[73] *University of the Punjab, Lahore-54590, Pakistan*
[74] *University of Turin and INFN, (A)University of Turin, I-10125, Turin, Italy; (B)University of Eastern Piedmont, I-15121, Alessandria, Italy; (C)INFN, I-10125, Turin, Italy*
[75] *Uppsala University, Box 516, SE-75120 Uppsala, Sweden*
[76] *Wuhan University, Wuhan 430072, People's Republic of China*
[77] *Yantai University, Yantai 264005, People's Republic of China*
[78] *Yunnan University, Kunming 650500, People's Republic of China*
[79] *Zhejiang University, Hangzhou 310027, People's Republic of China*
[80] *Zhengzhou University, Zhengzhou 450001, People's Republic of China*

[a] *Also at the Moscow Institute of Physics and Technology, Moscow 141700, Russia*
[b] *Also at the Novosibirsk State University, Novosibirsk, 630090, Russia*
[c] *Also at the NRC "Kurchatov Institute", PNPI, 188300, Gatchina, Russia*
[d] *Also at Goethe University Frankfurt, 60323 Frankfurt am Main, Germany*
[e] *Also at Key Laboratory for Particle Physics, Astrophysics and Cosmology, Ministry of Education; Shanghai Key Laboratory for Particle Physics and Cosmology; Institute of Nuclear and Particle Physics, Shanghai 200240, People's Republic of China*
[f] *Also at Key Laboratory of Nuclear Physics and Ion-beam Application (MOE) and Institute of Modern Physics, Fudan University, Shanghai 200443, People's Republic of China*
[g] *Also at State Key Laboratory of Nuclear Physics and Technology, Peking University, Beijing 100871, People's Republic of China*
[h] *Also at School of Physics and Electronics, Hunan University, Changsha 410082, China*
[i] *Also at Guangdong Provincial Key Laboratory of Nuclear Science, Institute of Quantum Matter, South China Normal University, Guangzhou 510006, China*
[j] *Also at MOE Frontiers Science Center for Rare Isotopes, Lanzhou University, Lanzhou 730000, People's Republic of China*
[k] *Also at Lanzhou Center for Theoretical Physics, Lanzhou University, Lanzhou 730000, People's Republic of China*
[l] *Also at the Department of Mathematical Sciences, IBA, Karachi 75270, Pakistan*

(Dated: **September 8, 2023**)

Based on 4.4 fb^{-1} of e^+e^- annihilation data collected at the center-of-mass energies between 4.60 and 4.70 GeV with the BESIII detector at the BEPCII collider, the pure W-exchange decay $\Lambda_c^+ \to \Xi^0 K^+$ is studied with a full angular analysis. The corresponding decay asymmetry is measured for the first time to be $\alpha_{\Xi^0 K^+} = 0.01 \pm 0.16(\text{stat.}) \pm 0.03(\text{syst.})$. This result reflects the interference between the S- and P-wave amplitudes. The phase shift between S- and P-wave amplitudes is $\delta_p - \delta_s = -1.55 \pm 0.25(\text{stat.}) \pm 0.05(\text{syst.})$ rad.

Investigations of charmed baryon decay dynamics are essential to explore the weak and strong interactions

in the Standard Model (SM) of particle physics. The ground state of the singly-charmed baryons, Λ_c^+, was discovered in 1979 [1]. Many studies have since been made of the properties of charmed baryons, such as the decay branching fractions (BFs) and decay asymmetries. But experimental results of the decay asymmetries, which are sensitive to the different amplitudes in the decay dynamics, have been limited. Since 2014, there has been some progress on the weak hadronic decays of Λ_c^+, $\Xi_c^{+,0}$, and Ω_c^0, both experimentally and theoretically [3, 4]. This provides crucial information about the properties of all the singly-charmed baryons and the searches for doubly-charmed baryons (Ξ_{cc} and Ω_{cc}) [5]. Nonetheless, the understanding of the decay dynamics of charmed baryons is still limited, due to the lack of precision experimental measurements and the difficulties in the theoretical treatment of strong interaction effects.

Compared to heavy meson decays, charmed baryon decays have a significant dependence on nonfactorizable contributions from W-exchange diagrams. However, these contributions cannot currently be calculated using theoretical approaches. Additionally, no experimental measurements exist for the decay asymmetries of W-exchange hadronic decays. An example of such a process is the decay $\Lambda_c^+ \to \Xi^0 K^+$, which can only be produced via a W-exchange process as depicted in Fig. 1. Experimental measurements of the asymmetry parameters of the decay $\Lambda_c^+ \to \Xi^0 K^+$ can aid understanding of the internal dynamics and can also explore charge-parity (CP) violation in baryons [5].
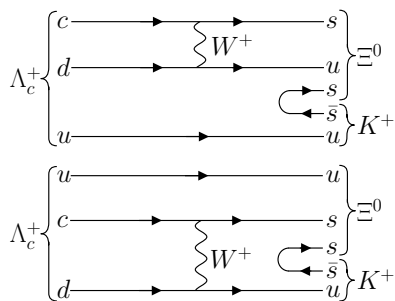

FIG. 1. Feynman diagrams for $\Lambda_c^+ \to \Xi^0 K^+$.

Table I lists the theoretical calculations of the BF and asymmetry parameters of $\Lambda_c^+ \to \Xi^0 K^+$, as well as the experimental measurements of the BF. Various predictions of the BFs based on the covariant confined quark model (CCQM), the pole model, and current algebra (CA) in the 1990s are all smaller than the experimental results [3]. This is explained as a strong cancellation in the S- and P-wave amplitudes. Moreover, the decay asymmetry parameter was predicted to be zero in these models owing to the vanishing S-wave amplitude [7–11]. This long-standing puzzle has recently experienced a renewed interest in the theoretical community [5, 12, 13], especially after the report of new

BF measured by BESIII in 2018 [14]. To reproduce the relatively large experimental branching fraction of this decay, Ref. [5] adopted a variant of the CA approach and obtained a larger $\mathcal{B}(\Lambda_c^+ \to \Xi^0 K^+) \simeq 0.71\%$. This modification introduces a large positive decay asymmetry of 0.90, which is quite close to the calculations based on SU(3) symmetry [12, 13]. However, regarding the significant enhancement of $\alpha_{\Xi^0 K^+}$ from 0 to about 0.9, the authors of Ref. [15] pointed out that the particular construction of the S-wave amplitude in Ref. [5] is not well-justified. So experimental measurement of the asymmetry parameter of the decay $\Lambda_c^+ \to \Xi^0 K^+$ will be crucial to test these calculations and confirm the vanishing S-wave contribution [15].

In the SM, the amplitude for a spin-1/2 baryon decaying into a spin-1/2 baryon and a spin-0 meson can be written as $M = i\bar{u}_f(A - B\gamma_5)u_i$, where A and B are constants, u_i and $\bar{u}_f$ are spinors describing the initial and final baryons [8]. For the decay $\Lambda_c^+ \to \Xi^0 K^+$, the decay asymmetry is defined by $\alpha_{\Xi^0 K^+} = 2\mathrm{Re}(s^*p)/(|s|^2 + |p|^2)$, where $s = A$ and $p = |\vec{p}_{\Xi^0}|B/(E_{\Xi^0} + m_{\Xi^0})$; here E_{Ξ^0} and $\vec{p}_{\Xi^0}$ are the energy and momentum of the Ξ^0 in the Λ_c^+ rest frame [3]. The effect of the S- and P-wave phase shift difference, $\delta_p - \delta_s$, is not well accounted for in the theoretical calculations of decay asymmetries. It can be extracted from experiments combined with the BF cited from the Particle Data Group (PDG) [3] and provides an important experimental parameter for the theoretical prediction of CP violation [16].

In this Letter, we present the first measurement of the decay asymmetry of $\Lambda_c^+ \to \Xi^0 K^+$ and its decay dynamic parameters ($|A|$, $|B|$, and $\delta_p - \delta_s$). A multidimensional angular analysis of the cascade-decay $e^+e^- \to \Lambda_c^+\bar{\Lambda}_c^-$, $\Lambda_c^+ \to \Xi^0 K^+$, $\Xi^0 \to \Lambda\pi^0$, and $\Lambda \to p\pi^-$ is performed using a technique similar to that used to measure the asymmetry parameters of $\Lambda_c^+ \to pK_S^0$, $\Lambda\pi^+$, $\Sigma^+\pi^0$, and $\Sigma^0\pi^+$ [17]. The data samples used in this analysis, with an integrated luminosity of 4.4 fb^{-1} [18], were collected at center-of-mass (CM) energies of 4.60, 4.63, 4.64, 4.66, 4.68, and 4.70 GeV with the BESIII detector at the BEPCII collider. Details about BEPCII as well as BESIII and its sub-detectors – a helium-based multilayer drift chamber (MDC), a plastic scintillator time-of-flight system (TOF), and a CsI(Tl) electromagnetic calorimeter (EMC) – can be found in Refs. [19–23]. Large data samples taken around the $\Lambda_c^+\bar{\Lambda}_c^-$ production threshold allow to measure decay asymmetry of low BF decays with the single-tag technique. The low-background environment is more favorable to measure $\alpha_{\Xi^0 K^+}$ accurately. Charge-conjugate modes are always implied unless explicitly stated otherwise.

Simulated event samples produced with a GEANT4-based [24] Monte Carlo (MC) package, which provides the geometric description of the BESIII detector and the detector response, are used to determine detection efficiencies and to estimate backgrounds. The simulation

TABLE I. Theoretical calculations and experimental measurements of the BF, $\alpha_{\Xi^0 K^+}$, $|A|$, $|B|$ and $\delta_p - \delta_s$ of $\Lambda_c^+ \to \Xi^0 K^+$. G_F is the Fermi constant. The superscript a denotes a model with SU(3) symmetry, while model b includes SU(3) symmetry-breaking effects. The PDG Fit BF also includes a CLEO result on $\mathcal{B}(\Lambda_c^+ \to \Xi^0 K^+)/\mathcal{B}(\Lambda_c^+ \to pK^-\pi^+)$ [3].

Theory or experiment	$\mathcal{B}(\Lambda_c^+ \to \Xi^0 K^+)$ ($\times 10^{-3}$)	$\alpha_{\Xi^0 K^+}$	$|A|$ ($\times 10^{-2} G_F$ GeV^2)	$|B|$ ($\times 10^{-2} G_F$ GeV^2)	$\delta_p - \delta_s$ (rad)
Körner (1992), CCQM [7]	2.6	0	-	-	-
Xu (1992), Pole [8]	1.0	0	0	7.94	-
Źencaykowski (1994), Pole [9]	3.6	0	-	-	-
Ivanov (1998), CCQM [10]	3.1	0	-	-	-
Sharma (1999), CA [11]	1.3	0	-	-	-
Geng (2019), SU(3) [12]	5.7 ± 0.9	$0.94^{+0.06}_{-0.11}$	2.7 ± 0.6	16.1 ± 2.6	-
Zou (2020), CA [5]	7.1	0.90	4.48	12.10	-
Zhong (2022), SU(3)^a [13]	$3.8^{+0.4}_{-0.5}$	$0.91^{+0.03}_{-0.04}$	3.2 ± 0.2	$8.7^{+0.6}_{-0.8}$	-
Zhong (2022), SU(3)^b [13]	$5.0^{+0.6}_{-0.9}$	0.99 ± 0.01	$3.3^{+0.5}_{-0.7}$	$12.3^{+1.2}_{-1.8}$	-
BESIII (2018) [14]	$5.90 \pm 0.86 \pm 0.39$	-	-	-	-
PDG Fit (2022) [3]	5.5 ± 0.7	-	-	-	-

models the beam energy spread and initial state radiation (ISR) in the e^+e^- annihilations with the generator KKMC [26, 27]. The inclusive MC sample includes the production of open charm processes, the ISR production of vector charmonium(-like) states, and the continuum processes incorporated in KKMC. All particle decays are modelled with EVTGEN [28, 29] using BFs either taken from the PDG [3], when available, or otherwise estimated with LUNDCHARM [30, 31]. Final state radiation from charged final state particles is incorporated using the PHOTOS package [32]. The phase space MC sample is generated uniformly over phase space, which is $e^+e^- \to \Lambda_c^+\bar{\Lambda}_c^-$ followed by $\Lambda_c^+ \to \Xi^0 K^+$, $\Xi^0 \to \Lambda(\to p\pi^-)\pi^0(\to \gamma\gamma)$ and $\bar{\Lambda}_c^-$ decaying inclusively. For the signal MC sample, the signal process is generated by the helicity formalism using the decay asymmetry parameters measured in this work or cited from the PDG [3].

The tracks of K^+ candidates detected in the MDC are required to be within a polar angle (θ) range of $|\cos\theta| < 0.93$, where θ is defined with respect to the z axis, which is the symmetry axis of the MDC. Besides, the distance of the closest approach to the interaction point (IP) must be less than 10 cm along the z axis, $|V_z|$, and less than 1 cm in the transverse plane, $|V_{xy}|$. The particle identification (PID) combining the dE/dx information from the MDC and the flight time from the TOF is implemented to evaluate the likelihoods $\mathcal{L}(h)$ ($h = \pi, K, p$) for different hadron hypotheses. Charged tracks satisfying $\mathcal{L}(K) > \mathcal{L}(\pi)$, and $\mathcal{L}(K) > 0$ are assigned as kaon candidates.

The π^0 candidates are formed by photon pairs with an invariant mass in the interval $0.115 < M_{\gamma\gamma} < 0.150$ GeV/c^2. The γ candidates are reconstructed from showers in the EMC that are not associated with any charged track. The deposited energy must be larger than 25 MeV in the barrel region ($|\cos\theta| < 0.80$) or 50 MeV in the end cap region ($0.86 < |\cos\theta| < 0.92$). To suppress electronic noise and showers unrelated to the event, the difference between the EMC time and the event start time is required to be within $[0, 700]$ ns. A mass-constrained fit to the known π^0 mass [3] is applied to the photon pair and the resulting energy and momentum of the π^0 is used for further analysis.

The Λ candidates are obtained from two oppositely charged tracks in the final states $p\pi^-$. Their distance of closest approaches to the IP must be within ± 20 cm along the beam direction. In order to improve signal purity, the proton PID is required to satisfy $\mathcal{L}(p) > \mathcal{L}(K)$, $\mathcal{L}(p) > \mathcal{L}(\pi)$ and $\mathcal{L}(p) > 0$. The two daughter tracks are constrained to originate from a common decay vertex by requiring the vertex fit χ^2 to be less than 20. The momentum of the Λ corrected by the vertex fit is used in subsequent analysis. Furthermore, the distance of the Λ decay vertex from the IP is required to be greater than twice the fitted vertex resolution. The $p\pi^-$ invariant mass is required to lie in the Λ mass region $(1.111, 1.121)$ GeV/c^2. The Ξ^0 candidates are formed by $\Lambda\pi^0$ combinations and the invariant mass $M_{\Lambda\pi^0}$ must be within the mass region $(1.30, 1.33)$ GeV/c^2. These mass regions are selected to be about three times the resolution.

Two kinematic variables, the energy difference $\Delta E \equiv E_{\Lambda_c^+} - E_{\text{beam}}$ and the beam-constrained mass $M_{\text{BC}} \equiv \sqrt{E_{\text{beam}}^2/c^4 - |\vec{p}_{\Lambda_c^+}|^2/c^2}$, are defined to identify $\Lambda_c^+ \to \Xi^0 K^+$ candidates. Here, $E_{\Lambda_c^+}$ and $\vec{p}_{\Lambda_c^+}$ are the reconstructed energy and momentum of the Λ_c^+ candidates calculated in the e^+e^- rest frame, and E_{beam} is the average energy of the e^+ and e^- beams. All candidates are required to satisfy $-0.05 < \Delta E < 0.05$ GeV and

2.25 GeV/c^2 < $M_{\rm BC}$ < $E_{\rm beam}$. If more than one candidate satisfies the above requirements, the one with minimal $|\Delta E|$ is kept. After applying these conditions, the $M_{\rm BC}$ distribution in data collected at 4.60 GeV is shown in the Fig. 2. In the fit to this data, the correctly and mis-reconstructed signal shapes are modeled with the MC-simulated shape convolved with a Gaussian function representing the resolution difference between data and MC simulation, and the background shape is described by an ARGUS function [33]. Finally, 378 ± 21 signal events are obtained by combining the six energy points.
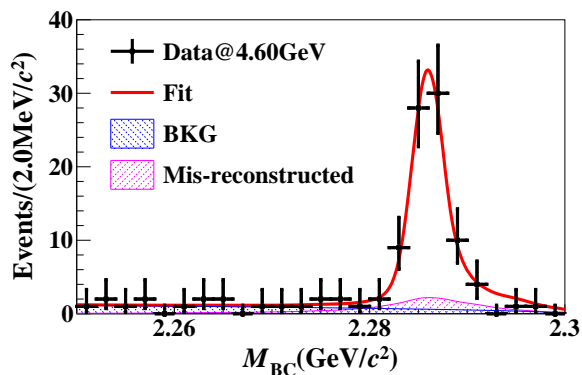

FIG. 2. Distribution of the $M_{\rm BC}$ fitting result at 4.60 GeV. Black points with error bars are data; the blue shaded region indicates the combinatorial background events and pink shaded region is the mis-reconstructed signal events.

The decay asymmetry parameters are determined by analyzing the multi-dimensional angular distributions, where the full cascade-decay chain is considered. The joint angular formula is obtained using helicity basis [34]. Figure 3 illustrates the definitions of the helicity angles for the three-level cascade decay $\Lambda_c^+ \to \Xi^0 K^+$, $\Xi^0 \to \Lambda\pi^0$, and $\Lambda \to p\pi^-$ following the process of $e^+e^- \to \gamma^* \to \Lambda_c^+\bar{\Lambda}_c^-$. In the helicity frame of the $e^+e^- \to \Lambda_c^+\bar{\Lambda}_c^-$, θ_0 is the polar angle of the Λ_c^+ with respect to the e^+ beam axis in the e^+e^- CM system. For the $\Lambda_c^+ \to \Xi^0 K^+$ decay, ϕ_1 is the angle between the $e^+\Lambda_c^+$ and $\Xi^0 K^+$ planes, and θ_1 is the polar angle of the Ξ^0 momentum in the Λ_c^+ rest frame with respect to the Λ_c^+ momentum in the CM frame. For the $\Xi^0 \to \Lambda\pi^0$ decay, ϕ_2 is the angle between the $\Xi^0 K^+$ and $\Lambda\pi^0$ planes, and θ_2 is the polar angle of the Λ momentum with respect to the Ξ^0 momentum in the rest frame of Λ_c^+. For the helicity angles describing the $\Lambda \to p\pi^-$ decay, ϕ_3 is the angle between the $\Lambda\pi^0$ and $p\pi^-$ planes, and θ_3 is the polar angle of the proton with respect to the Λ momentum in the Ξ^0 rest frame.

In Ref. [34], Δ_0 is defined as the phase shift between two individual helicity amplitudes, $\mathcal{H}_{\lambda_1, \lambda_2}$, for the Λ_c^+ production process $\gamma^* \to \Lambda_c^+(\lambda_1)\bar{\Lambda}_c^-(\lambda_2)$ with total helicities $|\lambda_1 - \lambda_2| = 0$ and 1, respectively. In the case where one-photon exchange dominates the production process, Δ_0 is also the phase between the
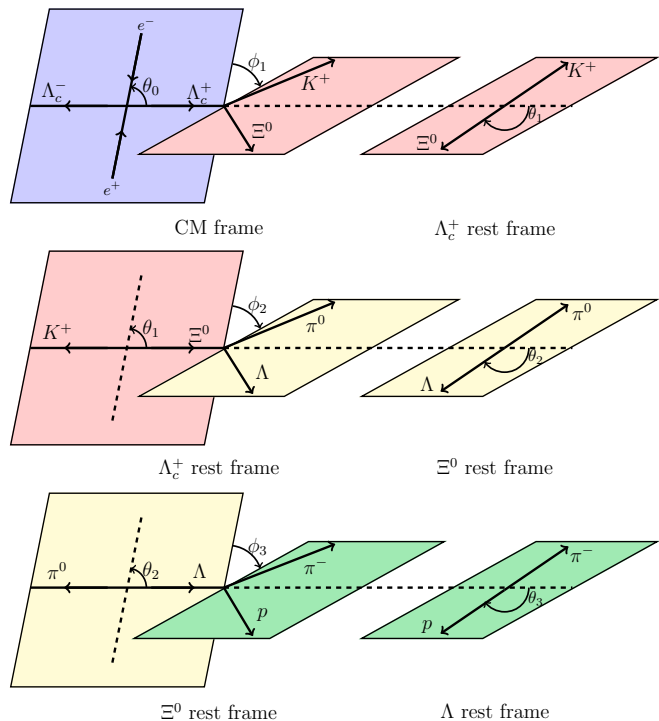

FIG. 3. Definitions of the helicity frames and related angles for $e^+e^- \to \Lambda_c^+\bar{\Lambda}_c^-$, $\Lambda_c^+ \to \Xi^0 K^+$, $\Xi^0 \to \Lambda\pi^0$, and $\Lambda \to p\pi^-$.

electric and magnetic form factors of Λ_c^+ [35, 36], and α_0 is the angular distribution parameter of Λ_c^+ defined by the helicity amplitude $\alpha_0 = (|\mathcal{H}_{1/2,-1/2}|^2 - 2|\mathcal{H}_{1/2,1/2}|^2)/(|\mathcal{H}_{1/2,-1/2}|^2 + 2|\mathcal{H}_{1/2,1/2}|^2)$. Similarly, the $\Lambda_c^+ \to \Xi^0 K^+$ decay is described by two parameters, $\alpha_{\Xi^0 K^+}$ and $\Delta_{\Xi^0 K^+}$, where the latter one is the phase shift between the two helicity amplitudes. The Lee-Yang parameters [1, 34] can be obtained with the relations

$$
\begin{aligned}
\beta_{\Xi^0 K^+} &= \sqrt{1 - (\alpha_{\Xi^0 K^+})^2} \, \sin\Delta_{\Xi^0 K^+}, \\
\gamma_{\Xi^0 K^+} &= \sqrt{1 - (\alpha_{\Xi^0 K^+})^2} \, \cos\Delta_{\Xi^0 K^+}.
\end{aligned}
\tag{1}
$$

In this analysis, the common free parameters ($\alpha_{\Xi^0 K^+}$ and $\Delta_{\Xi^0 K^+}$) describing the angular distributions for the six data sets are determined by a simultaneous unbinned maximum likelihood fit. The likelihood function is constructed from the joint probability density function (PDF) by

$$
\mathcal{L}_{\rm total} = \sum^{\rm energy} \mathcal{L}_{\rm data} = \prod_{i=1}^{N_{\rm data}} f_s(\vec{\xi}_i).
\tag{2}
$$

Here, $f_s(\vec{\xi}_i)$ is the PDF of the signal process, $N_{\rm data}$ is the number of events in data and i is the event index. The

signal PDF $f_s(\vec{\xi_i})$ is formulated as

$$f_s(\vec{\xi_i}) = \frac{\epsilon(\vec{\xi_i})|M(\vec{\xi_i};\vec{\eta})|^2}{\int \epsilon(\vec{\xi_i})|M(\vec{\xi_i};\vec{\eta})|^2 d\vec{\xi_i}} \ , \qquad (3)$$

where $\vec{\xi_i}$ denotes the kinematic angular observables ($\theta_{0,1,2,3}$ and $\phi_{1,2,3}$) and $\vec{\eta}$ denotes the free parameters ($\alpha_{\Xi^0 K^+}$ and $\Delta_{\Xi^0 K^+}$) to be determined. The $M(\vec{\xi_i};\vec{\eta})$ is the total decay amplitude [34] and $\epsilon(\vec{\xi_i})$ is the detection efficiency parameterized in terms of the kinematic variables $\vec{\xi_i}$. The background contribution to the joint likelihood is subtracted according to the calculated likelihoods for the combinatorial background based on the inclusive MC simulation and for the mis-reconstructed signal events based on the signal MC simulation. The integration of the normalization factor is calculated with a large phase space MC sample as

$$\int \epsilon(\vec{\xi_i})|M(\vec{\xi_i};\vec{\eta})|^2 d\vec{\xi_i} = \frac{1}{N_{\text{gen}}} \sum_{k_{\text{MC}}}^{N_{\text{MC}}} |M(\vec{\xi}_{k_{\text{MC}}};\vec{\eta})|^2 \ , \quad (4)$$

where N_{gen} is the total number of the simulated phase space MC events, N_{MC} is the number of the phase space MC events surviving all selection criteria and k_{MC} is the event index.

Using the MINUIT package [38], we minimize the negative logarithmic likelihood with background subtraction over the six data samples. Here, α_0, Δ_0, $\alpha_{\Lambda\pi^0}$, $\alpha_{\bar{\Lambda}\pi^0}$, $\Delta_{\Lambda\pi^0}$, and $\Delta_{\bar{\Lambda}\pi^0}$ are fixed to individual values measured by BESIII [39, 40], $\alpha_{p\pi^-}$ and $\alpha_{\bar{p}\pi^+}$ are fixed to the values from the PDG [3]. In the fit, $\alpha_{\Xi^0 K^+}$ and $\Delta_{\Xi^0 K^+}$ are free parameters, and $\alpha_{\Xi^0 K^+} = -\alpha_{\bar{\Xi}^0 K^-}$ and $\Delta_{\Xi^0 K^+} = -\Delta_{\bar{\Xi}^0 K^-}$ as required under the CP invariance assumption. The projections of the best fit onto several variables are shown in Fig. 4. The data are compared with the MC events weighted by the nominal fitting result. From this fit, we obtain $\alpha_{\Xi^0 K^+} = 0.01 \pm 0.16$ and $\Delta_{\Xi^0 K^+} = 3.84 \pm 0.90$ rad. Hence, the other two Lee-Yang parameters are calculated to be $\beta_{\Xi^0 K^+} = -0.64 \pm 0.69$ and $\gamma_{\Xi^0 K^+} = -0.77 \pm 0.58$, where the uncertainties are statistical only.

The systematic uncertainties arise mainly from the reconstruction of final state particles, which is studied with $J/\psi \to K_s^0 K^{\pm}\pi^{\mp}$ for kaon, $\Lambda_c^+ \to \Lambda X$ for Λ, $\psi(3686) \to J/\psi\pi^0\pi^0$ and $e^+e^- \to \omega\pi^0$ for π^0. For ΔE requirement and M_{BC} signal regions, which are estimated by smearing the phase space MC samples using resolution parameters. For the background subtraction, which is taking into account the background shape and size. The uncertainties from the quoted values of α_0, Δ_0, $\alpha_{\Lambda\pi^0}$, $\alpha_{\bar{\Lambda}\pi^0}$, $\Delta_{\Lambda\pi^0}$, $\Delta_{\bar{\Lambda}\pi^0}$, $\alpha_{p\pi^-}$ and $\alpha_{\bar{p}\pi^+}$ are estimated by Gaussian sampling considered their uncertainties and refit the angular distribution, and take the values in one time uncertainty of Gaussian fit as the uncertainties of this part. The fit bias, which is

the difference before and after the correction from pull distribution check. Systematic uncertainties from all sources are combined in quadrature to calculate the total systematic uncertainties. All systematic uncertainties are summarized in Table II and the relevant details can be found in Ref. [34].
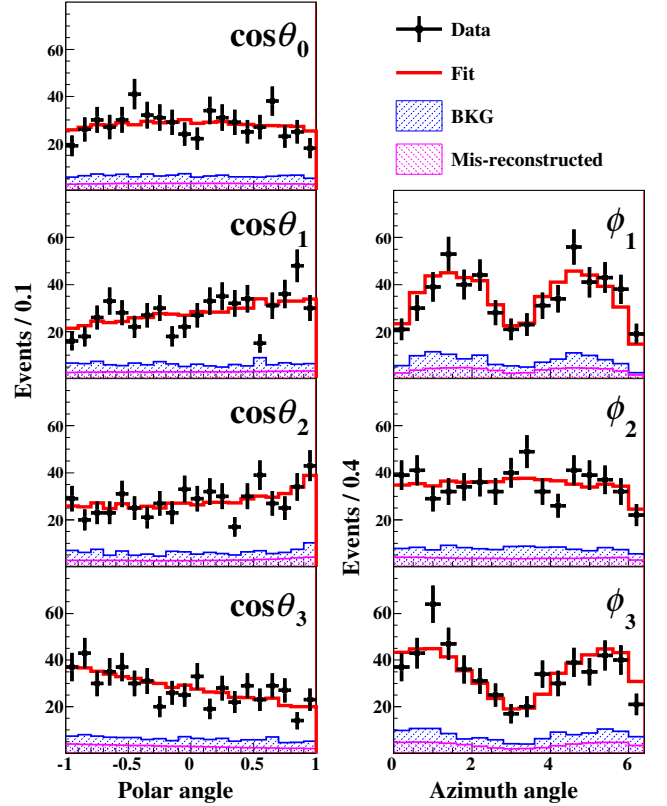

FIG. 4. Projections of the best fit onto various variables. Black points with error bars are data; red solid lines are phase space MC events re-weighted by angular distribution formula, and represent the fitting result; the blue shaded region denotes the combinatorial background events and the pink shaded region is the mis-reconstructed signal events.

TABLE II. Systematic uncertainties in $\alpha_{\Xi^0 K^+}$ and $\Delta_{\Xi^0 K^+}$.

Source	$\alpha_{\Xi^0 K^+}$	$\Delta_{\Xi^0 K^+}$[rad]
Tracking and PID efficiencies	negligible	negligible
π^0 reconstruction	negligible	negligible
Λ reconstruction	0.01	0.01
ΔE and M_{BC} signal regions	negligible	negligible
Background subtraction	0.03	0.08
Input parameters	0.01	0.14
Fit bias	negligible	0.05
Total	0.03	0.17

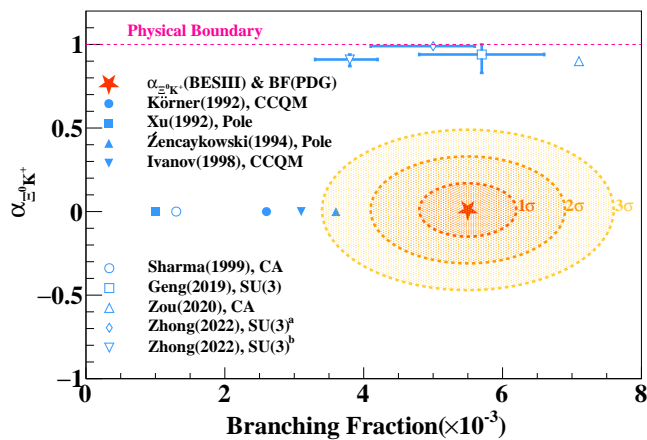The $\delta_p - \delta_s$ can be expressed by $\delta_p - \delta_s =$

FIG. 5. The comparison between this work and theoretical predictions, where the branching fraction is taken from PDG (2022) [3]. The blue symbols are theoretical predictions and the red star is result from this work. The definitions of the superscripts a and b can be found in Table I and the theory acronyms are explained in the text.

$\arctan(\sqrt{1 - \alpha_{\Xi^0 K^+}^2}\sin\Delta_{\Xi^0 K^+}/\alpha_{\Xi^0 K^+})$ and the derivation of $|A|$ and $|B|$ can be found in Ref. [34]. The study has uncovered two distinct physical solutions, with one group characterized by $|A| = 1.6^{+1.9}_{-1.6}$(stat.) $\pm$ 0.4(syst.) and $|B| = 18.3 \pm 2.8$(stat.) $\pm$ 0.7(syst.), and the other by $|A| = 4.3 \pm 0.7$(stat.) $\pm$ 0.2(syst.) and $|B| = 6.7^{+8.3}_{-6.7}$(stat.) $\pm$ 1.6(syst.).

In summary, by analyzing 4.4 fb^{-1} of e^+e^- annihilation data collected at the CM energies between 4.60 and 4.70 GeV with the BESIII detector, the pure W-exchange decay $\Lambda_c^+ \to \Xi^0 K^+$ from the $e^+e^- \to \Lambda_c^+ \bar{\Lambda}_c^-$ production has been studied. The decay asymmetry parameters are measured for the first time as $\alpha_{\Xi^0 K^+} = 0.01 \pm 0.16$(stat.)$\pm 0.03$(syst.) and $\Delta_{\Xi^0 K^+} = 3.84 \pm 0.90$(stat.)$\pm 0.17$(syst.) rad. The other two Lee-Yang parameters are calculated to be $\beta_{\Xi^0 K^+} = -0.64 \pm 0.69$(stat.)$\pm 0.13$(syst.) and $\gamma_{\Xi^0 K^+} = -0.77 \pm 0.58$(stat.) $\pm$ 0.11(syst.). The comparison between this work and theoretical predictions is shown in Fig. 5. Our measurement of $\alpha_{\Xi^0 K^+}$ is in good agreement with zero, which is consistent with the theoretical predictions from the 1990s. The decay dynamics parameters $|A|$, $|B|$, and $\delta_p - \delta_s$ are derived. The value of $\delta_p - \delta_s$ is observed to be -1.55 ± 0.25(stat.)± 0.05(syst.). This is of great significance for decay asymmetries, as $\cos(\delta_p - \delta_s)$ measured in this study is close to zero, an effect that had not been anticipated in previous literature. This measurement fills the long-standing puzzle and deepens our understanding of the strong dynamics in charmed baryon sector.

[1] G. S. Abrams, M. S. Alam, C. A. Blocker, A. Boyarski, M. Breidenbach, D. L. Burke, W. C. Carithers, W. Chinowsky, M. W. Coles and S. Cooper, et al. Phys. Rev. Lett. **44**, 10 (1980).
[2] R. L. Workman et al. (Particle Data Group), PTEP **2022**, 083C01 (2022).
[3] H. Y. Cheng, Chin. J. Phys. **78**, 324 (2022).
[4] H. Y. Cheng, Sci. Bull. **67**, 445 (2022).
[5] F. S. Yu, H. Y. Jiang, R. H. Li, C. D. Lü, W. Wang and Z. X. Zhao, Chin. Phys. C **42**, 051001 (2018).
[6] J. Zou, F. Xu, G. Meng and H. Y. Cheng, Phys. Rev. D **101**, 014011 (2020).
[7] J. G. Korner and M. Kramer, Z. Phys. C **55**, 659 (1992).
[8] Q. P. Xu and A. N. Kamal, Phys. Rev. D **46**, 270 (1992).
[9] P. Zenczykowski, Phys. Rev. D **50**, 5787 (1994).
[10] M. A. Ivanov, J. G. Korner, V. E. Lyubovitskij and A. G. Rusetsky, Phys. Rev. D **57**, 5632 (1998).

[11] K. K. Sharma and R. C. Verma, Eur. Phys. J. C **7**, 217 (1999).

[12] C. Q. Geng, C. W. Liu and T. H. Tsai, Phys. Lett. B **794**, 19 (2019).

[13] H. Zhong, F. Xu, Q. Wen and Y. Gu, JHEP **02**, 235 (2023).

[14] M. Ablikim *et al.* (BESIII Collaboration), Phys. Lett. B **783**, 200 (2018).

[15] S. Groote and J. G. Körner, Eur. Phys. J. C **82**, 297 (2022).

[16] J. P. Wang and F. S. Yu, arXiv:2208.01589 [hep-ph]

[17] M. Ablikim *et al.* (BESIII Collaboration), Phys. Rev. D **100**, 072004 (2019).

[18] M. Ablikim *et al.* (BESIII Collaboration), Chin. Phys. C **46**, no.11, 113003 (2022).

[19] M. Ablikim *et al.* (BESIII Collaboration), Nucl. Instrum. Meth. A **614**, 345 (2010).

[20] C. H. Yu *et al.*, Proceedings of IPAC2016, Busan, Korea, 2016.

[21] M. Ablikim *et al.* (BESIII Collaboration), Chin. Phys. C **44**, 040001 (2020).

[22] J. W. Zhang, L. H. Wu, S. S. Sun, J. H. Zou, C. X. Liu, Z. Y. Deng, Q. M. Ma, S. P. Wen, G. F. Cao and B. L. Zhang, *et al.* Rad. Det. Tech. Meth. **6**, no.3, 289-293 (2022).

[23] X. Li *et al.*, Rad. Det. Tech. Meth. **1**, 13 (2017); Y. X. Guo *et al.*, Rad. Det. Tech. Meth. **1**, 15 (2017); P. Cao *et al.*, Nucl. Instrum. Meth. A **953**, 163053 (2020).

[24] S. Agostinelli *et al.* (GEANT4 Collaboration), Nucl. Instrum. Meth. A **506**, 250 (2003).

[25] K. X. Huang, Z. J. Li, Z. Qian, J. Zhu, H. Y. Li, Y. M. Zhang, S. S. Sun and Z. Y. You, Nucl. Sci. Tech. **33**, 142 (2022).

[26] S. Jadach, B. F. L. Ward and Z. Was, Phys. Rev. D **63**, 113009 (2001).

[27] S. Jadach, B. F. L. Ward and Z. Was, Comput. Phys. Commun. **130**, 260 (2000).

[28] D. J. Lange, Nucl. Instrum. Meth. A **462**, 152 (2001).

[29] R. G. Ping, Chin. Phys. C **32**, 599 (2008).

[30] J. C. Chen, G. S. Huang, X. R. Qi, D. H. Zhang and Y. S. Zhu, Phys. Rev. D **62**, 034003 (2000).

[31] R. L. Yang, R. G. Ping and H. Chen, Chin. Phys. Lett. **31**, 061301 (2014).

[32] E. Richter-Was, Phys. Lett. B **303**, 163 (1993).

[33] H. Albrecht *et al.* [ARGUS], Phys. Lett. B **241**, 278-282 (1990).

[34] See Supplemental Material attached to the end of the passage for the Lee-Yang parameters, joint angular distribution formula, details of the systematic uncertainties, and the relation with weak decay amplitude.

[35] G. Fäldt, Phys. Rev. D **97**, 053002 (2018).

[36] M. Ablikim *et al.* (BESIII Collaboration), Phys. Rev. Lett. **120**, 132001 (2018).

[37] T. D. Lee and C. N. Yang, Phys. Rev. **108**, 1645 (1957).

[38] F. James and M. Roos, Comput. Phys. Commun. **10**, 343 (1975).

[39] M. Ablikim *et al.* (BESIII Collaboration), arXiv:2307.07316 [hep-ex]

[40] M. Ablikim *et al.* (BESIII Collaboration), Phys. Rev. D **108**, no.3, L031106 (2023)

Supplemental Material for "First Measurement of the Decay Asymmetry of pure W-exchange Decay $\Lambda_c^+ \to \Xi^0 K^+$"

i. DECAY ASYMMETRY PARAMETERS

For the process $e^+e^- \to \Lambda_c^+ \bar{\Lambda}_c^-$, $\Lambda_c^+ \to BP$ and $\bar{\Lambda}_c^-$ decaying to anything, where B and P denote a $J^P = \frac{1}{2}^+$ baryon and a $J^P = 0^-$ pseudoscalar meson, respectively, the amplitude can be constructed using the helicity basis. For the weak non-leptonic decay $\Lambda_c^+ \to BP$, the Lee-Yang variables [1] α_{BP}, β_{BP} and γ_{BP} are defined with respect to the s-wave and p-wave amplitudes, such as

$$\alpha_{BP} = \frac{2\text{Re}(s^*p)}{|s|^2 + |p|^2}, \quad \beta_{BP} = \frac{2\text{Im}(s^*p)}{|s|^2 + |p|^2}, \quad \gamma_{BP} = \frac{|s|^2 - |p|^2}{|s|^2 + |p|^2}, \tag{i.1}$$

where s and p are the parity-odd and parity-even decay amplitudes. In a non-relativistic picture, they correspond to the L = 0 (S-wave) and L = 1 (P-wave) orbital angular momenta of the baryon-meson system, respectively.

The parameters α_{BP}, β_{BP}, and γ_{BP} satisfy

$$\alpha_{BP}^2 + \beta_{BP}^2 + \gamma_{BP}^2 = 1. \tag{i.2}$$

We work with helicity amplitudes. For $\Lambda_c^+ \to B(\frac{1}{2}^+) P(0^-)$ decays, we have two helicity amplitudes, $\mathcal{H}_{\frac{1}{2}}$ and $\mathcal{H}_{-\frac{1}{2}}$. Using the relations $s = \frac{1}{\sqrt{2}}(\mathcal{H}_{\frac{1}{2}} + \mathcal{H}_{-\frac{1}{2}})$, $p = \frac{1}{\sqrt{2}}(\mathcal{H}_{\frac{1}{2}} - \mathcal{H}_{-\frac{1}{2}})$, the asymmetry parameters defined with helicity amplitudes are

$$\begin{aligned}
\alpha_{BP} &= |\mathcal{H}_{\frac{1}{2}}|^2 - |\mathcal{H}_{-\frac{1}{2}}|^2, \\
\beta_{BP} &= \sqrt{1 - \alpha_{BP}^2}\sin\Delta_{BP}, \\
\gamma_{BP} &= \sqrt{1 - \alpha_{BP}^2}\cos\Delta_{BP},
\end{aligned} \tag{i.3}$$

where we take the normalization $|\mathcal{H}_{\frac{1}{2}}|^2 + |\mathcal{H}_{-\frac{1}{2}}|^2 = 1$, and Δ_{BP} is the phase angle difference between two helicity amplitudes $\mathcal{H}_{\frac{1}{2}}$ and $\mathcal{H}_{-\frac{1}{2}}$.

If the Λ_c^+ and $\bar{\Lambda}_c^-$ decays respect CP symmetry, we have relations between the Λ_c^+ and $\bar{\Lambda}_c^-$ asymmetry parameters

$$\alpha_{\bar{B}\bar{P}} = -\alpha_{BP}, \ \beta_{\bar{B}\bar{P}} = -\beta_{BP}, \ \gamma_{\bar{B}\bar{P}} = \gamma_{BP}. \tag{i.4}$$

ii. JOINT ANGULAR DISTRIBUTION FORMULA FOR THE DECAY $\Lambda_c^+ \to \Xi^0 K^+$

In the helicity frame of the $e^+e^- \to \Lambda_c^+ \bar{\Lambda}_c^-$ system, θ_0 is the polar angle of the Λ_c^+ with respect to the e^+ beam axis in the e^+e^- CM system. For the $\Lambda_c^+ \to \Xi^0 K^+$ decay, ϕ_1 is the angle between the $e^+\Lambda_c^+$ and $\Xi^0 K^+$ planes and θ_1 is the polar angle of the Ξ^0 momentum in the Λ_c^+ rest frame with respect to the Λ_c^+ momentum in the CM frame. For the helicity system describing $\Xi^0 \to \Lambda\pi^0$ decay, ϕ_2 is the angle between the $\Xi^0 K^+$ and $\Lambda\pi^0$ planes and θ_2 is the polar angle of the Λ momentum with respect to the Ξ^0 momentum in the rest frame of Λ_c^+. For the helicity angles describing the $\Lambda \to p\pi^-$ decay, ϕ_3 is the angle between the $\Lambda\pi^0$ and $p\pi^-$ planes and θ_3 is the polar angle of the proton with respect to the Λ momentum in the Ξ^0 rest frame. In the $\Lambda_c^+ \to \Xi^0 K^+$ process, as shown in Table I, λ_1, λ_2, λ_3, λ_4 and λ_5 indicate the helicity of Λ_c^+, $\bar{\Lambda}_c^-$, Ξ^0, Λ and p. A_{λ_1,λ_2}, B_{λ_3}, C_{λ_4} and D_{λ_5} are the helicity amplitudes.

TABLE I. Definition of decays, helicity angles and amplitudes, where λ_i indicates the helicity values for the corresponding hadron.

Level	Decay	Helicity angle	Helicity amplitude
0	$e^+e^- \to \Lambda_c^+(\lambda_1)\,\bar{\Lambda}_c^-(\lambda_2)$	(θ_0)	A_{λ_1,λ_2}
1	$\Lambda_c^+ \to \Xi^0(\lambda_3)\,K^+$	(θ_1,ϕ_1)	B_{λ_3}
2	$\Xi^0 \to \Lambda(\lambda_4)\,\pi^0$	(θ_2,ϕ_2)	C_{λ_4}
3	$\Lambda \to p(\lambda_5)\,\pi^-$	(θ_3,ϕ_3)	D_{λ_5}

The joint angular distribution is defined as

$$
\frac{d\Gamma}{d\cos\theta_0 \, d\cos\theta_1 \, d\cos\theta_2 \, d\cos\theta_3 \, d\phi_1 \, d\phi_2 \, d\phi_3}
$$

$$
\propto \sum_{\lambda_1,\lambda_2,\lambda_3,\lambda_4,\lambda_5} \rho^{\lambda_1-\lambda_2,\lambda_1'-\lambda_2}(\theta_0) \, D^{\frac{1}{2}\,*}_{\lambda_1,\lambda_3}(\theta_1,\phi_1,0) \, D^{\frac{1}{2}}_{\lambda_1',\lambda_3}(\theta_1,\phi_1,0) \, B_{\lambda_3} \, B^{*}_{\lambda_3'} \tag{ii.1}
$$

$$
D^{\frac{1}{2}\,*}_{\lambda_3,\lambda_4}(\theta_2,\phi_2,0) \, D^{\frac{1}{2}}_{\lambda_3',\lambda_4'}(\theta_2,\phi_2,0) \, C_{\lambda_4} \, C^{*}_{\lambda_4'} \, D^{\frac{1}{2}\,*}_{\lambda_4,\lambda_5}(\theta_3,\phi_3,0) \, D^{\frac{1}{2}}_{\lambda_4',\lambda_5}(\theta_3,\phi_3,0) \, |D_{\lambda_5}|^2,
$$

where $\rho^{\lambda_1-\lambda_2,\lambda_1'-\lambda_2}(\theta_0) = \sum_{M=\pm 1} d^1_{M,\lambda_1-\lambda_2}(\theta_0) \, d^1_{M,\lambda_1'-\lambda_2}(\theta_0) \, A_{\lambda_1,\lambda_2} \, A^{*}_{\lambda_1',\lambda_2}$ corresponds to the Λ_c^+ spin density matrix and $D^J_{m,n}(\phi,\theta,\gamma) = e^{-im\phi} \, d^J_{m,n}(\theta) \, e^{-in\gamma}$ is Wigner-D function [2]. The helicity amplitudes A_{λ_1,λ_2} are related to the asymmetry parameters $\alpha_0 = \dfrac{\left|A_{\frac{1}{2},-\frac{1}{2}}\right|^2 - 2\left|A_{\frac{1}{2},\frac{1}{2}}\right|^2}{\left|A_{\frac{1}{2},-\frac{1}{2}}\right|^2 + 2\left|A_{\frac{1}{2},\frac{1}{2}}\right|^2}$, and helicity B_{λ_3} is related to the asymmetry parameter $\alpha_{\Xi^0 K^+} = $

$\dfrac{\left|B_{\frac{1}{2}}\right|^2 - \left|B_{-\frac{1}{2}}\right|^2}{\left|B_{\frac{1}{2}}\right|^2 + \left|B_{-\frac{1}{2}}\right|^2}$, helicity C_{λ_4} is related to the asymmetry parameter $\alpha_{\Lambda\pi^0} = \dfrac{\left|C_{\frac{1}{2}}\right|^2 - \left|C_{-\frac{1}{2}}\right|^2}{\left|C_{\frac{1}{2}}\right|^2 + \left|C_{-\frac{1}{2}}\right|^2}$ and helicity D_{λ_5} is related

to the asymmetry parameter $\alpha_{p\pi^-} = \dfrac{\left|D_{\frac{1}{2}}\right|^2 - \left|D_{-\frac{1}{2}}\right|^2}{\left|D_{\frac{1}{2}}\right|^2 + \left|D_{-\frac{1}{2}}\right|^2}$. Then the joint angular distribution becomes

$$
\frac{d\Gamma}{d\cos\theta_0 \, d\cos\theta_1 \, d\cos\theta_2 \, d\cos\theta_3 \, d\phi_1 \, d\phi_2 \, d\phi_3}
$$

$$
\propto 1 + \alpha_0\cos^2\theta_0
$$
$$
+ (1 + \alpha_0\cos^2\theta_0) \, \alpha_{\Xi^0 K^+} \alpha_{\Lambda\pi^0} \cos\theta_2
$$
$$
+ (1 + \alpha_0\cos^2\theta_0) \, \alpha_{\Xi^0 K^+} \alpha_{p\pi^-} \cos\theta_2\cos\theta_3
$$
$$
+ (1 + \alpha_0\cos^2\theta_0) \, \alpha_{\Lambda\pi^0} \alpha_{p\pi^-} \cos\theta_3
$$
$$
- (1 + \alpha_0\cos^2\theta_0) \, \alpha_{\Xi^0 K^+} \sqrt{1-\alpha_{\Lambda\pi^0}^2} \, \alpha_{p\pi^-} \sin\theta_2\sin\theta_3\cos(\Delta_{\Lambda\pi^0} + \phi_3)
$$
$$
+ \sqrt{1-\alpha_0^2} \, \sin\Delta_0\sin\theta_0\cos\theta_0\alpha_{\Xi^0 K^+} + \sin\theta_1\sin\phi_1
$$
$$
+ \sqrt{1-\alpha_0^2} \, \sin\Delta_0\sin\theta_0\cos\theta_0\alpha_{\Lambda\pi^0}\sin\theta_1\sin\phi_1\cos\theta_2
$$
$$
+ \sqrt{1-\alpha_0^2} \, \sin\Delta_0\sin\theta_0\cos\theta_0\alpha_{\Xi^0 K^+}\alpha_{\Lambda\pi^0}\alpha_{p\pi^-}\sin\theta_1\sin\phi_1\cos\theta_3
$$
$$
+ \sqrt{1-\alpha_0^2} \, \sin\Delta_0\sin\theta_0\cos\theta_0\alpha_{p\pi^-}\sin\theta_1\sin\phi_1\cos\theta_2\cos\theta_3
$$
$$
- \sqrt{1-\alpha_0^2} \, \sin\Delta_0\sin\theta_0\cos\theta_0\sqrt{1-\alpha_{\Lambda\pi^0}^2} \, \alpha_{p\pi^-}\sin\theta_1\sin\phi_1\sin\theta_2\sin\theta_3\cos(\Delta_{\Lambda\pi^0} + \phi_3)
$$
$$
+ \sqrt{1-\alpha_0^2} \, \sin\Delta_0\sin\theta_0\cos\theta_0\sqrt{1-\alpha_{\Xi^0 K^+}^2} \, \alpha_{\Lambda\pi^0}\cos\phi_1\sin\theta_2\sin(\Delta_{\Xi^0 K^+} + \phi_2)
$$
$$
+ \sqrt{1-\alpha_0^2} \, \sin\Delta_0\sin\theta_0\cos\theta_0\sqrt{1-\alpha_{\Xi^0 K^+}^2} \, \alpha_{\Lambda\pi^0}\cos\theta_1\sin\phi_1\sin\theta_2\cos(\Delta_{\Xi^0 K^+} + \phi_2)
$$
$$
+ \sqrt{1-\alpha_0^2} \, \sin\Delta_0\sin\theta_0\cos\theta_0\sqrt{1-\alpha_{\Xi^0 K^+}^2} \, \alpha_{p\pi^-}\cos\theta_1\sin\phi_1\sin\theta_2\cos(\Delta_{\Xi^0 K^+} + \phi_2)\cos\theta_3
$$
$$
+ \sqrt{1-\alpha_0^2} \, \sin\Delta_0\sin\theta_0\cos\theta_0\sqrt{1-\alpha_{\Xi^0 K^+}^2} \, \alpha_{p\pi^-}\cos\phi_1\sin\theta_2\sin(\Delta_{\Xi^0 K^+} + \phi_2)\cos\theta_3
$$
$$
- \sqrt{1-\alpha_0^2} \, \sin\Delta_0\sin\theta_0\cos\theta_0\sqrt{1-\alpha_{\Xi^0 K^+}^2}\sqrt{1-\alpha_{\Lambda\pi^0}^2} \, \alpha_{p\pi^-}\cos\theta_1\sin\phi_1\sin(\Delta_{\Xi^0 K^+} + \phi_2)\sin\theta_3\sin(\Delta_{\Lambda\pi^0} + \phi_3)
$$
$$
+ \sqrt{1-\alpha_0^2} \, \sin\Delta_0\sin\theta_0\cos\theta_0\sqrt{1-\alpha_{\Xi^0 K^+}^2}\sqrt{1-\alpha_{\Lambda\pi^0}^2} \, \alpha_{p\pi^-}\cos\theta_1\sin\phi_1\cos\theta_2\cos(\Delta_{\Xi^0 K^+} + \phi_2)\sin\theta_3\cos(\Delta_{\Lambda\pi^0} + \phi_3)
$$
$$
+ \sqrt{1-\alpha_0^2} \, \sin\Delta_0\sin\theta_0\cos\theta_0\sqrt{1-\alpha_{\Xi^0 K^+}^2}\sqrt{1-\alpha_{\Lambda\pi^0}^2} \, \alpha_{p\pi^-}\cos\phi_1\cos(\Delta_{\Xi^0 K^+} + \phi_2)\sin\theta_3\sin(\Delta_{\Lambda\pi^0} + \phi_3)
$$
$$
+ \sqrt{1-\alpha_0^2} \, \sin\Delta_0\sin\theta_0\cos\theta_0\sqrt{1-\alpha_{\Xi^0 K^+}^2}\sqrt{1-\alpha_{\Lambda\pi^0}^2} \, \alpha_{p\pi^-}\cos\phi_1\cos\theta_2\sin(\Delta_{\Xi^0 K^+} + \phi_2)\sin\theta_3\cos(\Delta_{\Lambda\pi^0} + \phi_3)
$$

$$\tag{ii.2}$$

where the α_0 is the angular distribution parameter of $e^+e^- \to \Lambda_c^+\bar{\Lambda}_c^-$ and Δ_0 is the transverse polarization for Λ_c^+. The decay asymmetry parameters $\alpha_{\Lambda\pi^0}$ and $\alpha_{p\pi^-}$ are taken from PDG [3]. The $\Delta_{\Xi^0 K^+} = \delta^B_{\frac{1}{2}} - \delta^B_{-\frac{1}{2}}$ and $\Delta_{\Lambda\pi^0} = \delta^C_{\frac{1}{2}} - \delta^C_{-\frac{1}{2}}$ are the difference of the phase of the helicity amplitude B and C, respectively. For the charge conjugate mode, $\bar{\Lambda}_c^- \to \bar{\Xi}^0 K^-$, the formula of angular distribution is same.

iii. SYSTEMATIC UNCERTAINTY

The systematic uncertainties arise mainly from the reconstruction of final states, ΔE requirement, M_{BC} signal selection, the background subtraction, the uncertainties from the quoted values of α_0, Δ_0, $\alpha_{\Lambda\pi^0}$, $\alpha_{\bar{\Lambda}\pi^0}$, $\Delta_{\Lambda\pi^0}$, $\Delta_{\bar{\Lambda}\pi^0}$, $\alpha_{p\pi^-}$, and $\alpha_{\bar{p}\pi^+}$, and the fit bias. Systematic uncertainties from various sources are combined in quadrature to calculate the total systematic uncertainties.

The reconstruction efficiency of charged kaon is studied with the control sample of $J/\psi \to K_S^0 K^{\pm}\pi^{\mp}$ events, that for π^0 with $\psi(3686) \to \pi^0\pi^0 J/\psi$ and $e^+e^- \to \omega\pi^0$, and that for Λ with $J/\psi \to \bar{p}K^+\Lambda$ and $J/\psi \to \Lambda\bar{\Lambda}$ [4]. The signal MC samples are re-weighted based on the data-MC differences in various momentum ranges resulting in new MC integration and new fitting parameters. The uncertainties related to the ΔE and M_{BC} requirement are evaluated by smearing the signal MC sample with a Gaussian resolution function. The changes of the fit results based on new accepted signal MC events are taken as the systematic uncertainties. All effects mentioned above are negligible except for Λ reconstruction.

For the background subtraction, we consider both background size and the background modelling. The background size including combinational background and mis-reconstructed component is obtained from the fit to the M_{BC} spectrum. The relevant systematic uncertainties are examined by repeating the fits with a alternative background size obtained from the Gaussian sampling of the fitted parameters. The ensemble of fitted parameters obtained will be fit to a Gaussian and the sum of the fitted Gaussian resolution and the difference between the fitted Gaussian mean and the nominal result are assigned as the systematic uncertainty for background size. The uncertainty of the background modelling also considers both combinational background and the mis-reconstructed component. The mis-reconstructed model is examined by an alternative signal MC sample produced with the new input parameters $\alpha_{\Xi^0 K^+}$ and $\Delta_{\Xi^0 K^+}$ which are changed within $\pm 1\sigma$. The uncertainty due to the combinational background model is estimated by varying the relative weights between $\Lambda_c^+\bar{\Lambda}_c^-$ pairs and other hadronic events based on the uncertainties of their cross section ratio.

The systematic uncertainty due to the input parameters is evaluated by varying these parameters within $\pm 1\sigma$ using a Gaussian sampling method. For each parameter, the obtained results are fit to a Gaussian function and the sum of the fitted Gaussian resolution and the difference between the fitted Gaussian mean and the nominal result is taken as the systematic uncertainty. The systematic uncertainties arising from fit bias are investigated via pull distribution checks. The mean values of the pull distributions are used to correct the nominal results. The differences between the uncorrected and corrected results are assigned as systematic uncertainties.

All systematic uncertainties discussed above are summarized in Table II.

TABLE II. Systematic uncertainties in $\alpha_{\Xi^0 K^+}$ and $\Delta_{\Xi^0 K^+}$.

Source	$\alpha_{\Xi^0 K^+}$	$\Delta_{\Xi^0 K^+}[\mathrm{rad}]$
Tracking and PID efficiencies	negligible	negligible
π^0 reconstruction	negligible	negligible
Λ reconstruction	0.01	0.01
ΔE and M_{BC} signal regions	negligible	negligible
Background subtraction	0.03	0.08
Input parameters	0.01	0.14
Fit bias	negligible	0.05
Total	0.03	0.17

iv. RELATION WITH WEAK DECAY AMPLITUDE

In the Standard Model, the amplitude for the two-body weak decay $\Lambda_c^+ \to \Xi^0 K^+$ can be parameterized as $\mathcal{M} = i\bar{u}_{\Xi^0}(A - B\gamma_5)u_{\Lambda_c^+}$, based on the S-wave and P-wave amplitudes, $s = A$ and $p = \kappa B$ [3]. Combination the Eq. (i.1) and the relationship between the $\mathcal{B}(\Lambda_c^+ \to \Xi^0 K^+)$ and the amplitude, the decay width and decay asymmetry can be

obtained as follows:

$$\Gamma = \frac{\mathcal{B}(\Lambda_c^+ \to \Xi^0 K^+)}{\tau_{\Lambda_c^+}} = \frac{|\vec{p}_c|}{8\pi}\left[\frac{(m_{\Lambda_c^+} + m_{\Xi^0})^2 - m_{K^+}^2}{m_{\Lambda_c^+}^2}|A|^2 + \frac{(m_{\Lambda_c^+} - m_{\Xi^0})^2 - m_{K^+}^2}{m_{\Lambda_c^+}^2}|B|^2\right],$$

$$\alpha_{\Xi^0 K^+} = \frac{2\kappa|A||B|\cos(\delta_p - \delta_s)}{|A|^2 + \kappa^2|B|^2}, \tag{iv.1}$$

$$\Delta_{\Xi^0 K^+} = \arctan\frac{2\kappa|A||B|\sin(\delta_p - \delta_s)}{|A|^2 - \kappa^2|B|^2},$$

with $\kappa = |\vec{p}_c|/(E_{\Xi^0} + m_{\Xi^0}) = \sqrt{(E_{\Xi^0} - m_{\Xi^0})/(E_{\Xi^0} + m_{\Xi^0})} \approx 0.234582$ and $\vec{p}_c$ is the momentum of the Ξ^0 baryon in the rest frame of Λ_c^+ particle [5].

Upon solving the system of equations presented in Eq. (iv.1), an exquisite solution can be obtained. The complexity of the solution is such that its exposition is not suitable here.

––––––––––

[1] T. D. Lee and C. N. Yang, Phys. Rev. **108**, 1645 (1957).
[2] Sachs, Robert G., Science **130**, 1106 (1959).
[3] R. L. Workman *et al.* [Particle Data Group], PTEP **2022**, 083C01 (2022).
[4] M. Ablikim *et al.* (BESIII Collaboration), Phys. Rev. Lett. **121**, 062003 (2018).
[5] J. Zou, F. Xu, G. Meng and H. Y. Cheng, Phys. Rev. D **101**, 014011 (2020).